

---

# Synthesis and Characterisation of DOTA-Kisspeptin-10 as a Potential Gallium-68/Lutetium-177 Theranostic Radiopharmaceutical

---

[Janke Kleynhans](#) , Robert Reeve , [Cathryn HS Driver](#) , [Biljana Marjanovic-Painter](#) , [Mike M Sathekge](#) , [Jan Rijn Zeevaart](#) , [Thomas Ebenhan](#) , [Robert P Millar](#) \*

Posted Date: 23 April 2024

doi: 10.20944/preprints202404.1446.v1

Keywords: Theranostics; Peptide Receptor Radionuclide Therapy (PRRT); antimetastatic; Radiopharmaceutical; Positron Emission Computed Tomography (PET); Pharmacokinetics; Pharmacodynamics; tumorigenesis



Preprints.org is a free multidiscipline platform providing preprint service that is dedicated to making early versions of research outputs permanently available and citable. Preprints posted at Preprints.org appear in Web of Science, Crossref, Google Scholar, Scilit, Europe PMC.

Copyright: This is an open access article distributed under the Creative Commons Attribution License which permits unrestricted use, distribution, and reproduction in any medium, provided the original work is properly cited.

Disclaimer/Publisher's Note: The statements, opinions, and data contained in all publications are solely those of the individual author(s) and contributor(s) and not of MDPI and/or the editor(s). MDPI and/or the editor(s) disclaim responsibility for any injury to people or property resulting from any ideas, methods, instructions, or products referred to in the content.

Article

# Synthesis and Characterisation of DOTA-Kisspeptin-10 as a Potential Gallium-68/Lutetium-177 Theranostic Radiopharmaceutical

Janke Kleynhans <sup>1</sup>, Robert Reeve <sup>2</sup>, Cathryn HS Driver <sup>1,3</sup>, Biljana Marjanovic-Painter <sup>3</sup>, Mike Sathekge <sup>1,4</sup>, Jan Rijn Zeevaart <sup>1,3</sup>, Thomas Ebenhan <sup>1,3,4</sup> and Robert P Millar <sup>2,\*</sup>

<sup>1</sup> NuMeRI, Nuclear Medicine Research Infrastructure NPC, South Africa

<sup>2</sup> Centre for Neuroendocrinology, University of Pretoria, South Africa

<sup>3</sup> The South African Nuclear Energy Corporation (NECSA), South Africa

<sup>4</sup> Department of Nuclear Medicine and Steve Biko Academic Hospital, University of Pretoria, South Africa

\* Correspondence: bob.millar@up.ac.za

**Abstract:** Kisspeptin (KISS1) and its cognate receptor (KISS1R) are implicated in the progression of various cancers. However, a theranostic radiopharmaceutical targeting the KISS1 receptor (KISS1R) has yet to be explored. A gallium-68 labelled kisspeptin-10 (KP10) has potential as a pan-tumor radiopharmaceutical for the detection of cancers. Furthermore, a lutetium-177 labelled KP10 could find therapeutic application in treating oncological diseases. We attached DOTA to the NH<sub>2</sub>-terminus of KP10 as we posited that this modification would not impair biological activity and showed that receptor stimulation of inositol phosphate accumulation in HEK293 transfected with the KISS1R gene was similar for KP10 and DOTA-KP10. We describe optimization of radiolabeling with gallium-68 and lutetium-177 and stability in serum, plasma, and whole blood. Pharmacokinetics was established with  $\mu$ PET/CT and ex vivo measurements. Dynamic studies with  $\mu$ PET/CT demonstrated that background clearance for the radiopharmaceutical was rapid with a blood half-life of  $18 \pm 3$  minutes. DOTA-KP10 demonstrated preserved functionality at KISS1R and good blood clearance. These promising results advocate the further development of KP10 structures which have high binding affinity along with proteolytic resistance.

**Keywords:** Theranostics; Peptide Receptor Radionuclide Therapy (PRRT); antimetastatic; Radiopharmaceutical; Positron Emission Computed Tomography (PET); Pharmacokinetics; Pharmacodynamics; tumorigenesis

## 1. Introduction

There is growing evidence that tumorigenesis is influenced by the antimetastatic kisspeptin gene (KISS1 gene) [1–8] that encodes pro-kisspeptin which is proteolytically cleaved to kisspeptin-54, kisspeptin-14, kisspeptin-13, and kisspeptin-10. All the cleaved kisspeptins are biologically active and have the same 10 amino acid carboxyl terminus sequence. The KISS1 gene and KISS1 receptor (KISS1R) display variable mRNA expression levels in different cancers and at different cancer stages [1]. This offers an opportunity to explore the development of a novel kisspeptin theranostic radiopharmaceutical targeting a variety of tumor types.

A major biologically active product of the kisspeptin precursor is Kisspeptin-10 (KP10) [1–4]. KP-10 together with KISS1R has been observed to display a stimulatory or inhibitory role in tumors depending on the type of cancer. In some tumor types, the KISS1R/KISS1 pathway is upregulated in the primary tumor and serves as a tumorigenesis and metastasis suppressor [2,4]. Contrarily, in other tumor types, it is widely expressed in metastases and leads to an increase in progression and poorer prognosis [2,3]. This apparent contradiction/conundrum is also characteristic of other mediators in cancer such as NF $\kappa$ B, c-MYC, AMP-activated protein kinase, transforming growth factor  $\beta$ , SKY and hyaluronidase that have been demonstrated to fulfil dual roles [2]. The application of the KISS1R as

a target in the clinical setting therefore appears to depend on the type of primary tumor and KISS1R expression profile [2]. The potential roles of KISS/KISS1R expression in different tumor types is summarized in Figure 1, updated from the review by Guzman et al., [2]. Radionuclide labelled kisspeptin peptides therefore provide a potential target for diagnostic imaging and if proven efficacious, might have application as a therapeutic radiopharmaceutical (theranostic).

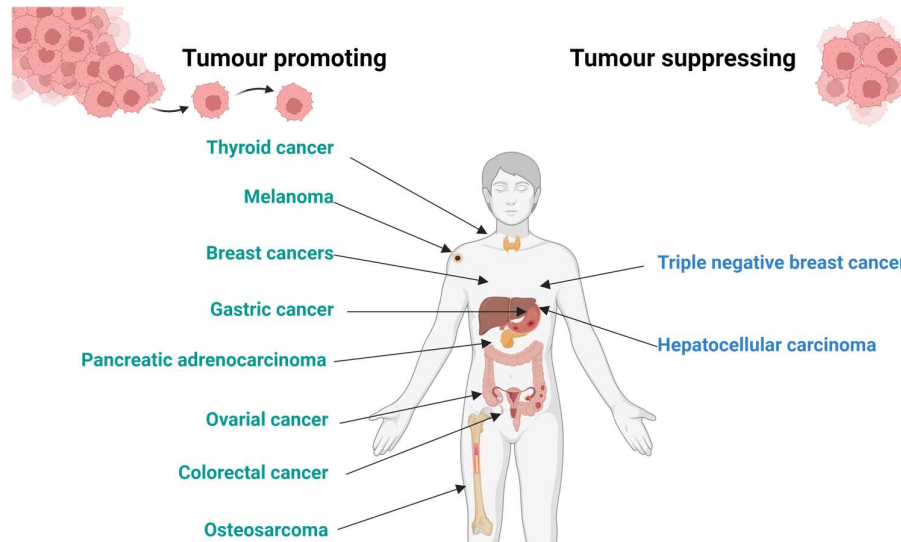


**Figure 1.** Tumor promoting and tumor suppressing sites in human tissues (drawn with licensed version of BioRender.com) [2,5–8].

In the development of a kisspeptin theranostic agent (a KP10 derivative), a diagnostic and therapeutic radionuclide along with an appropriate chelator needs to be selected. The choice of gallium-68 as a diagnostic nuclide is logical because of the logistics and convenience associated with its clinical use, as described previously [9,10]. The combination of therapeutic radionuclide, lutetium-177, along with gallium-68 presents a theranostic partnership as demonstrated by gallium-68 or lutetium-177 labelled PSMA used in clinical practice. The optimal chelator choice for this nuclide is the widely used and approved DOTA (1,4,7,10-tetraazacyclododecane-*N,N',N'',N'''*- tetraacetic acid) [11].

As a sight for conjugation of DOTA to KP10 we chose the NH<sub>2</sub>-terminus as this is extended in the natural kisspeptins and our studies on modification of this site show it is well tolerated [11–13]. The addition of DOTA at the NH<sub>2</sub>-terminus it was unlikely to hinder the key binding/activation residues, Phe6, Arg9 and Phe10. These residues play an important role in accessing the hydrophobic pocket of the KISS1R receptor [14]. The literature also indicates that Asn4, Ser5, Gly7, Arg9 and Phe10 are involved in binding and activity of KP10 at the KISS1R [15].

We proposed that [<sup>68</sup>Ga]Ga-DOTA-KP10 would be efficacious (illustrated in Appendix A). As shown for other [<sup>68</sup>Ga]Ga-DOTA peptides lutetium-177 labelling would potentially serve as a therapeutic but also for surgical debulking in primary tumors where KISS1R has a tumor suppression effect. It could also provide [<sup>177</sup>Lu]Lu-DOTA-KP10 therapy for breast cancer and hepatocellular carcinoma where metastases express the KISS1R [2,5,6].

The current study aimed to optimize the radiolabeling of DOTA-KP10 to produce [<sup>68</sup>Ga]Ga-DOTA-KP10 and [<sup>177</sup>Lu]Lu-DOTA-KP10 using a simple and repeatable procedure.

## 2. Results

### 2.1. Inositol Phosphate Accumulation Assay

To determine if the functionalization of KP10 with DOTA (for radiolabeling) was not influencing activity at the KISS1R receptor, the functional signaling assay of inositol phosphate accumulation was performed. This is a measure of the ligand binding and receptor activation. The EC<sub>50</sub>'s of KP10 and

DOTA-KP10 were determined as  $\sim 1.87 \times 10^{-9}$  M and  $3.994 \times 10^{-9}$  M, respectively from four independent experiments (Table 1). The maximal response to DOTA-KP10 was 97.8% of that of KP10 (Figure 2).

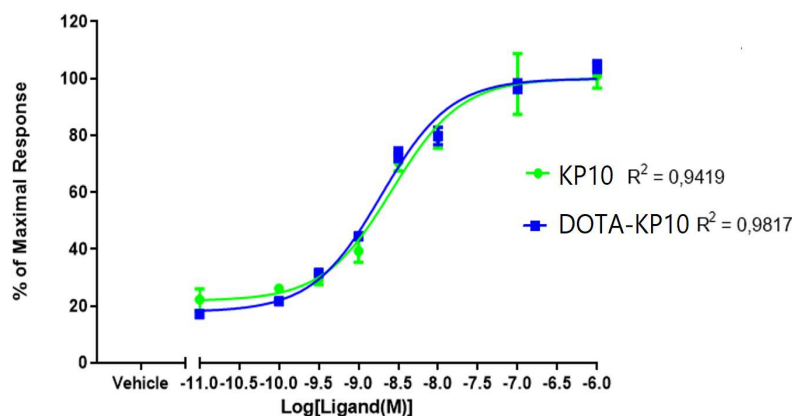


**Figure 2.** Stimulation of inositol phosphates accumulation in cells expressing KISS1R by the DOTA-KP10 ligand and native KP10. Data points were fitted by sigmoidal dose response curves and are presented as a percentage of the maximal response of KP10 (set at 100%). Data are expressed as mean and SD (N=5).

**Table 1.** The effective concentrations which elicited a 50% maximal response in HEK 293-T cells expressing KISS1R when treated with KP10 and DOTA-KP10. The data are represented as a mean with the standard error mean for a sample size of four. The values were not significantly different.

Ligand	EC <sub>50</sub> Mean nM ± SEM (N=4)
KP10	1.87 ± 0.095
DOTA-KP-10	3.99 ± 0.075

## 2.2. Radiolabeling Optimization and Radiochemical Purity

The optimal radiosynthesis method identified for labelling of DOTA-KP10 with gallium-68 features a compound concentration of 10  $\mu$ M incubated at a pH of 4.0 for 10 minutes at 95 °C. The analysis of radiochemical purity was performed by ITLC and confirmed with HPLC for all samples in the case of gallium-68. For <sup>177</sup>Lu-labelling only radio-HPLC analysis was performed. Individual chromatogram examples are provided in Appendix B.

For all animal studies, a well-established product purification was performed using a C18 SepPak cartridge to ensure desalting, change of activity concentration and a radiochemical purity of more than 95% [16]. For labelling of DOTA-KP10 with lutetium-177, only the compound molarity was investigated. It was determined that high and robust radiolabeling efficiency was achieved using compound molarity of 20-25  $\mu$ M. Detailed results with regards to radiolabeling optimization are provided in Appendix C.

## 2.3. Log P Octanol/Phosphate Buffered Assay

The accumulation of [<sup>68</sup>Ga]Ga-DOTA-KP10 in the aqueous phase was 99.1 ± 0.72% (N=5) with a Log P value of -2.0. This demonstrates that the compound is very water-soluble.

## 2.4. Ex Vivo Stability

The benchtop stability of [<sup>68</sup>Ga]Ga-DOTA-KP10 (N=3) formulated in PBS over a 3 h period remained unchanged (>95%) confirmed by various sampling points. The <sup>177</sup>Lu-based radiopharmaceutical demonstrated equal stability with a 100% radiochemical purity measured in various samples of [<sup>177</sup>Lu]Lu-DOTA-KP10 (N=3) up to 24 hours. Individual chromatogram examples are provided in Appendix D.

The red blood cell binding assay demonstrated that the binding of [<sup>68</sup>Ga]Ga-KP10 was 6.72 ± 0.37%. The [<sup>68</sup>Ga]Ga-KP10 associated radioactivity bound to the plasma proteins increased gradually over time with 28.2 ± 1.35 % after initiating the incubation, 46.4 ± 7.24 % after 1 hour and 67.99 ± 3.56%

at 2 hours of incubation (N=3). When exposed to whole blood, serum and plasma, [ $^{68}\text{Ga}$ ]Ga-DOTA-KP10 showed the formation of a degradation product on the radio-chromatogram evident in the 5 min samples (Figure 3B, C, D). Although the product was not quantified nor identified, some instability and interaction are present. Stability was measured over time (5 min incubation, 1 hour and 2 hours, N=3).

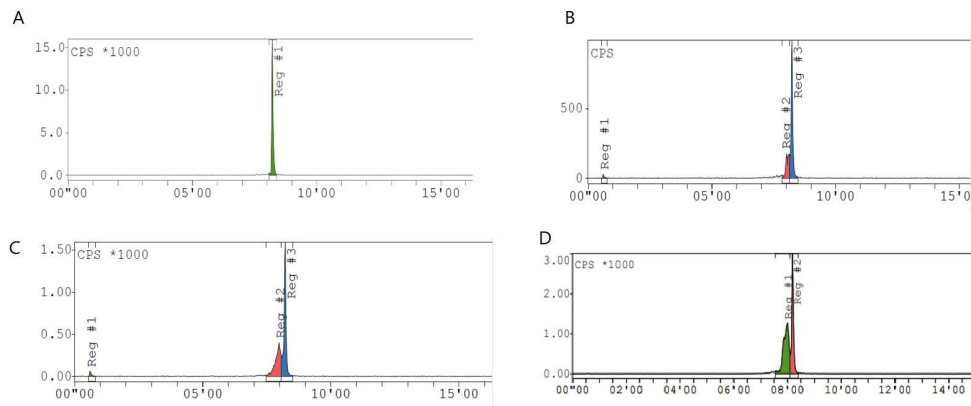


**Figure 3.** Example chromatograms of [ $^{68}\text{Ga}$ ]Ga-DOTA-KP10: control not incubated with biological samples (A) and samples at 5 minutes after addition to plasma (B), serum (C) or whole blood (D) which showed the greatest production of the unknown metabolite. The changes seen in the radio-chromatograms by radio-HPLC were not quantified or further identified.

### 2.5. In Vivo Evaluation and Ex-Vivo Biodistribution

Dynamic uptake studies with microPET/CT after [ $^{68}\text{Ga}$ ]Ga-DOTA-KP10 administration on bed indicated that the background clearance of this radiopharmaceutical was rapid. A blood half-life of  $18 \pm 3$  min was calculated (Figure 4). At 120 minutes radioactivity was still excreted as visualised by an elevated bladder signal (and kidneys) (Figure 5). Based on the visual qualitative data, it is not perceived that the radiopharmaceutical will be persistent in the kidneys. Ex vivo organ radioactivity was analysed and used for %ID/g calculation (Figure 6); no organs accumulated the radiopharmaceutical significantly (< 0.5% ID/g, except for kidneys ( $1.5 \pm 0.2\%$  ID/g)). Activity presence in the kidneys was maintained at 150 minutes as well as noticeable activity in the stomach (low but largely variable).

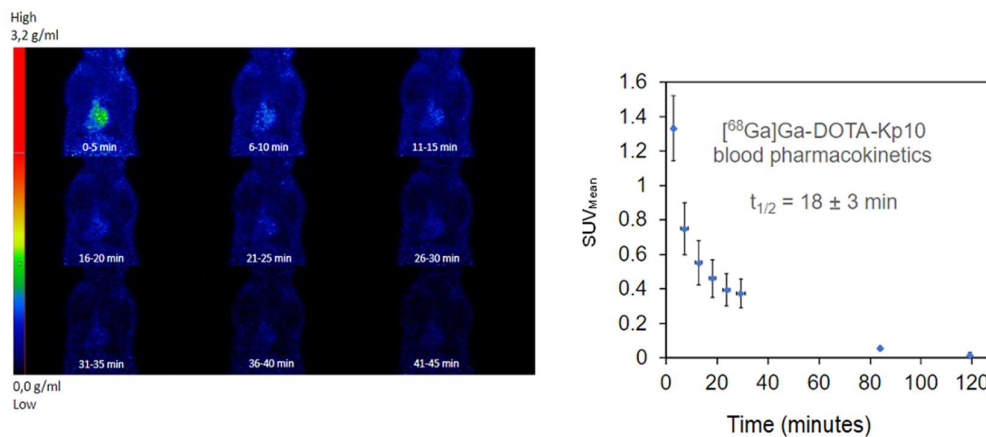


**Figure 4.** Display of dynamic PET imaging represented by different coronal cross sections (A) showing a gradual decrease of blood pool activity over 34 minutes; the image-guided (CT based region of interest of the myocardium, N=4) SUV analysis was performed to draw time-activity curve (B) to allow for calculation of the physiological half-life of [ $^{68}\text{Ga}$ ]Ga-DOTA-KP10 ( $R^2 = 0.895$ ).

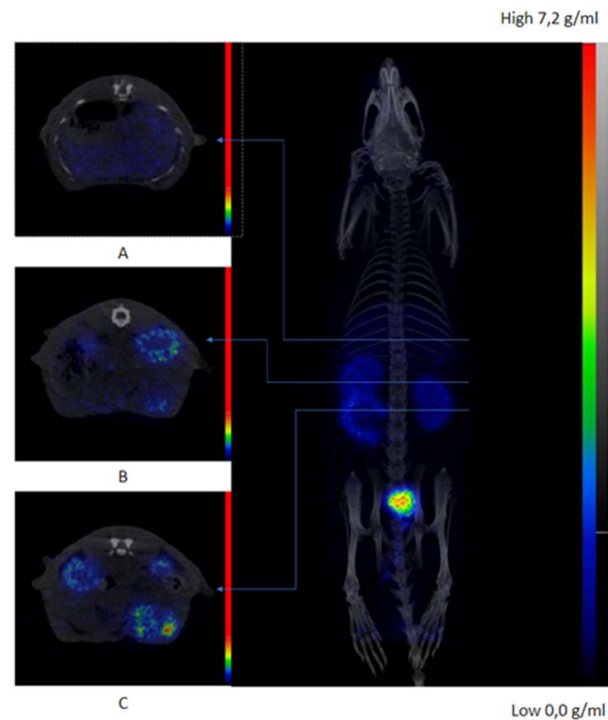


**Figure 5.** An exemplary full body image in maximum intensity projection from a 120 minutes delayed microPET/CT acquisition (right) with cross sectional PET/CT image slices (right panel) demonstrating noticeable radioactive in A) liver, B) right kidney, C) left kidney and small intestine.

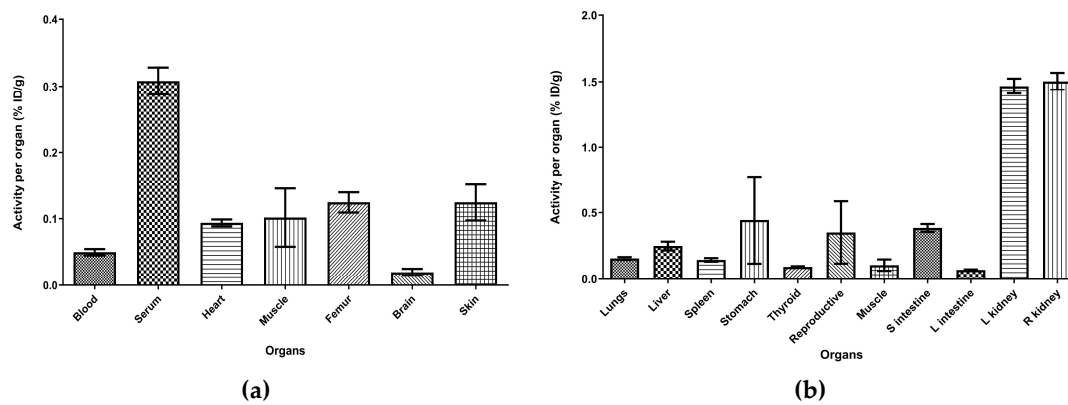


**Figure 6.**  $[^{68}\text{Ga}]\text{Ga-DOTA-KP10}$  biodistribution derived from ex-vivo gamma counting of dissected organs at 150 minutes post-injection. Results are presented as % injected dose per gram. Data are expressed as mean and SD (N=5).

### 3. Discussion

The original discovery of differential expression of KISS1R in metastatic and non-metastatic melanoma cell lines sparked extensive studies on the relationship of KP and KISS1R in numerous cancers which found a diversity of results in cancers; many of which were contradictory [1–8]. To further understand the complexity of the KP/ KISS1R involvement in cancer a radiolabeled KP could be utilized as a biomarker to visualize KISS1R expression in vivo which may prospectively be used in non-invasive cancer diagnosis or monitoring therapeutic response with PET/CT imaging. In particular, it provides the opportunity to clarify and resolve the role of KP in cancer progression; for example in triple-negative breast cancer and hepatocellular carcinoma  $[^{68}\text{Ga}]\text{Ga-DOTA-KP10}$  could be predictive of a more aggressive disease and as a theranostic,  $[^{177}\text{Lu}]\text{Lu-DOTA-KP10}$  could open unexplored avenues for radioligand therapy. The current investigation provides initial steps in the

feasibility towards developing such a radiopharmaceutical as there have not been any studies on the use of KP10 derivatives for intravenous administration and in vivo imaging or radiotherapy.

Our study presents robust data demonstrating that KP-10 conjugated to DOTA via the NH<sub>2</sub>-terminus retains full biological activity. This concurs with SAR studies, which demonstrated that structural modification at the NH<sub>2</sub>-terminus of KP10 did not impair receptor binding and activation [11–14].

The investigation also achieved robust radiosynthesis procedures for the complexation of gallium-68 or lutetium-177 which proceeded well in line with other PRRT peptides. Both gallium-68 and lutetium-177 radiolabeling optimizations resulted in a product with a radiochemical purity higher than 95%, both meeting the release criteria for molar activity, activity concentration and radiochemical yield and total yield/radiosynthesis. The optimal radiolabeling molarity for lutetium-177 was > 20  $\mu$ M when employing similar conditions as those used for <sup>68</sup>Ga-labelling (pH 4.5, 95°C, 10 min). Encouragingly, no formation of radiolysis products or other impurities were present during stability assays of the formulated products (pH 7) at room temperature (approximately 25°C). These [<sup>68</sup>Ga]Ga-DOTA-KP10 samples were stable sufficiently long to dispense and analyze multiple doses (2 hours) and [<sup>177</sup>Lu]Lu-DOTA-KP10 was stable over a 24 hour duration. To this end, developing a molecule further for theranostic purposes, should require that the measurement period for stability verification be increased to 72 hours after radiopharmaceutical production.

The [<sup>68</sup>Ga]Ga-DOTA-KP10 protein binding was found to be moderate within the first hour (23%) which favored a rapid renal compound clearance. The physiological half-life was determined in vivo in healthy rodents and was deemed acceptable for further investigations. It demonstrates a quick clearance of non-targeted radiopharmaceutical.

The amount of the radiopharmaceutical associated with red blood cells was demonstrated to be negligible. A gradual but moderate formation of an additional radioactive peak preceding the main product peak was detected during radio-HPLC analysis of [<sup>68</sup>Ga]Ga-DOTA-KP10 incubated in human serum, plasma and whole blood. No further investigations were undertaken, mainly because KP10 (Tyr-Asn-Trp-Asn-Ser-Phe-Gly-Leu-Arg-Phe) is a linear peptide known to be susceptible to proteolytic breakdown or nucleophilic attack. In a study by Takeda pharmaceuticals, the COOH-terminal peptide bond between Arg<sup>9</sup>-Phe<sup>10</sup> was degradable by trypsin-like proteases and the Tyr<sup>1</sup>-Asn<sup>2</sup> amino acid pair underwent NH<sub>2</sub>-terminal degradation by aminopeptidases [17]. The intrapeptidyl cleavage areas at Gly<sup>7</sup> may be vulnerable towards chymotrypsin-like proteases, neutral endopeptidases, and matrix metalloproteases [26]. Additionally, asparagine residues (here Asn<sup>2</sup>) have been shown to undergo spontaneous rearrangement in aqueous environments [19–21]. Hence, these amino acid (Tyr<sup>1</sup>, Asn<sup>2</sup>, Gly<sup>7</sup>, and Arg<sup>9</sup>) may account for the serum instability. Instability can be addressed by the substitution of the vulnerable amino acids by D-amino acids and unnatural synthetic amino acids - a viable approach which is extensively employed for biological peptides. This has already been established in the structure of TAK 448 [21]. Conjugation of this compound with a DOTA-derivatized NH<sub>2</sub>-terminus and other enhanced-activity KP10 agonists are likely to deliver increased activity and diminished degradation.

This study is the first to design and characterize DOTA labelled KP-10 and undertake the in vivo characteristics and pharmacokinetics of radiolabeled KP10 using dynamic PET/CT for its visualization in healthy rats. These results demonstrated a decrease in blood pool activity of [<sup>68</sup>Ga]Ga-DOTA-KP10 primarily through avid renal excretion with no visible, unexpected off-target organ accumulation of activity. From this exploratory study design, a six to eight-fold serum: blood ratio was established from ex vivo sample gamma counting. Gamma analysis indicated that the radiopharmaceutical may also show signs of kidney retention, which in the light of cancer theranostics, should be further investigated. The microPET/CT image analysis showed uniform distribution of activity in neovasculature and soft tissue over the 45 min dynamic scan period with no noticeable accumulation (other than elevated perfusion) in the brain or lungs. Delayed, [<sup>68</sup>Ga]Ga-DOTA-KP10 PET/CT images were acquired (at 120-145 min) for a whole-body representation of tracer biodistribution, thereby showing no vascular retention, lung or brain uptake with clearance through the expected excretory passages (renal > hepatobiliary). These observations were confirmed with the ex vivo organ distribution.

## 4. Materials and Methods

### 4.1. Materials

The 1850 MBq germanium-68 generator was obtained from iThemba LABS (Somerset West, South Africa). Hydrochloric acid 0.6 M for elution was obtained from ABX biopharmaceuticals GmbH (Radeberg, Germany). Lutetium-177 (n.c.a) was obtained from NTP Radioisotopes SOC Ltd (Hartebeespoort, South Africa). Certified DOTA-KP10 was synthesized by GL Biochem (Shanghai, China) with the attachment of DOTA at the NH<sub>2</sub>-terminus of KP10 with a molecular weight of 1688.43 g/mol and a purity of 96% (structure available in Supplementary Data A). All solvents, reagents and materials used during the synthesis and radiochemical analysis (supra-pure HCl, trifluoroacetic acid, ethanol, acetonitrile, sodium acetate trihydrate, sodium citrate, pH test strips and Millex GV 0.22 µm sterile filters) were purchased from Sigma-Aldrich (Darmstadt, Germany) or Merck (Kenilworth, New Jersey, USA). Deionized, ultrapure water was produced with a Simplicity 185 Millipore system (Cambridge, USA). The C18 SepPak cartridges for post-purification were available from Waters (Milford, USA). Phosphate Buffered Saline from ABX (Radeberg, Germany) was used for the final formulation. Materials for the cell culture assay were XtremeGene HP DNA transfection reagent from Roche Diagnostics (Basel, Switzerland), matrigel from Corning Life Sciences (New York, USA), DMEM, high glucose, GlutaMAX™ from Thermo Fisher Scientific (Waltham, USA) and trypsin-EDTA solution from Sigma Aldrich (Sigma-Aldrich, St Louis, MO, USA). Cell culture plates and other flasks were obtained from Corning Life Sciences (New York, USA). Human embryonic kidney (HEK) 293-T cells were obtained from ATCC (Manassas, VA, USA). Dowex 100-200 mesh was sourced from Sigma-Aldrich (Darmstadt, Germany), Media-199 was obtained from Thermo Fisher Scientific, myo-inositol and scintillation liquid from Perkin Elmer (Waltham, MA, USA).

### 4.2. Methods

#### 4.2.1. HEK Cell Culture Preparation and Inositol Phosphate Accumulation Assay

HEK 293-T cell culturing and the inositol phosphate (IP) accumulation assay were performed as described by Newton et al. [16,17]. The IP assay measures the response of the cells to ligands which is a measure of the binding affinity and stimulation of intracellular signaling and used to determine whether the novel ligand retained the same activity as KP10.

HEK 293-T cells were cultured and maintained using DMEM (10% FBS) media supplemented with Glutamax at 37 °C, 5% CO<sub>2</sub>- and 95% relative humidity. HEK 293-T cells were passaged at 90% confluency using Trypsin. HEK 293-T cells were plated out into 24 well plates at a density of 1x10<sup>5</sup> -cells /well. Each well was pre-coated with Matrigel at a 1:30 dilution to ensure adhesion to the well. KISS1R gene construct was transiently transfected into the HEK 293-T cells at a concentration of 10 ng/µl of KISS1R using XtremeGene HP (1:2 ratio) DNA transfection reagent. Cells were incubated overnight at 37 °C at 5 % CO<sub>2</sub>.

For the IP assay, the HEK 293-T cells were incubated with myo-inositol-[2-3H] (3H-myo-inositol) (0.55 µCi/well) in IP Media (Medium-199 supplemented with 1% FBS) at 37 °C for 16 hours. The IP medium was subsequently aspirated off and the cells incubated in Buffer I (140mM NaCl, 4mM KCl, 20mM HEPES, 8mM glucose, 0.1% SA, 1mM MgCl<sub>2</sub>, 1mM CaCl<sub>2</sub>) supplemented with 10mM LiCl<sub>2</sub> for 30 minutes followed by a one-hour incubation at 37 °C with the ligands (unconjugated KP10 and DOTA-KP10) in Buffer I. Following stimulation of the cells with the peptides, the cells were lysed for 1 hour in 10 mM formic acid at 4 °C. The radiolabeled inositol phosphates were separated using a Dowex 100-200 mesh resin ion-exchange chromatography and the radioactivity (cpm) was measured using liquid scintillation (Packard Tricarb 2100 TR liquid scintillation analyser TRI-CARB 4910TR 110 V Liquid Scintillation Counter, Perkin-Elmer, USA). The experiment was done in triplicate and the three repeats were averaged. The results were analyzed by doing sigmoidal regression to determine the EC 50 and then compared to their respective normalized ligand signaling assay.

The accumulation of the inositol phosphates measured for cells transfected with XtremeGene without KISS1R and treated with a maximal stimulation of KP10 (1x10<sup>-6</sup> M) was subtracted from the measured accumulation of cells stimulated with DOTA-KP10 over a dose range (1x10<sup>-11</sup> - 1x10<sup>-6</sup> M) which were transfected with KISS1R in the same assay.

#### 4.2.2. Radiolabeling Optimization

The iThemba LABS  $^{68}\text{Ge}/^{68}\text{Ga}$ -generator (1.85 GBq, 1-month-old) was eluted by fractionated elution as described previously to reduce the concentration of contaminants that can influence radiolabelling efficiency [24]. The  $^{68}\text{Ga}$ -radiolabelling parameters for DOTA-KP10 were based on a previously published procedure by us [25]. In brief, eluate acidity, compound molarity, incubation time and temperature were evaluated. All labelling reactions were performed using a 1.0  $\mu\text{g}/\mu\text{l}$  peptide-chelator stock solutions (deionised water) comparing temperatures of 25 °C (room temperature), 60 °C and 95 °C. The reactions were monitored at 5-minute intervals over a 20-minute period by determining the radiochemical purity as described in Section 2.2.4. Further radiolabelling was evaluated over a range of peptide-chelator concentrations (5  $\mu\text{M}$  to 25  $\mu\text{M}$ ) and at pH ranging from 3.0 - 5.0 (note: effect of pH was evaluated at suboptimal peptide concentration (5  $\mu\text{M}$ ) to ensure that any variations in the radiolabelling efficiency were clearly seen).

The preliminary evaluation of labelling of DOTA-KP10 with lutetium-177 was aimed at demonstrating the possibility of development of a theranostic radiopharmaceutical. A method for  $^{177}\text{Lu}$ -labelling suggested by Sinnes et al., was therefore followed and not further optimised [26]. Non-carrier added lutetium-177 in 0.5 M HCl (100 MBq =  $\pm$  0.1 nmol) was used and DOTA is capable of complexing lutetium-177 in molar ratios from 1:5 to 1:10 (lutetium-177: chelator) for reproducible, quantitative labelling. Labelling was performed using 100 MBq lutetium-177 (2-4 days old) added to 1 ml of DOTA-KP10 (variable concentrations) and at a pH of 4.5 for 5 min. The temperature was kept constant at 95° C. After labelling was performed, the final product was buffered to a pH of 7 with 2.5 M sodium citrate for the stability study.

#### 4.2.3. Product Purification for in Vivo Analysis

To ensure that the product was >99% pure for further biological applications, [ $^{68}\text{Ga}$ ]Ga-DOA-KP10 was purified as previously described [24]. In brief, a C18 SepPak cartridge was conditioned with ethanol (>99.5%) and equilibrated with Millipore deionized water. The reaction product was loaded on the cartridge, washed, and eluted with 1:1 (ethanol: saline). No more than 10% ethanol was used in final preparation. In preparation for administration into animals, the ethanol contents were minimized by evaporation.

#### 4.2.4. Radiochemical Purity Analysis

Instant thin-layer chromatography (ITLC) was performed as described previously using silica-gel TLC paper (ITLC-SG). Each TLC was evaluated using two mobile phases: 0.1 M sodium citrate (pH 5.0) solution for determining the ionic (free)  $^{68}\text{Ga}$ -species; and a mixture of 50:50 1M ammonium acetate/methanol to determine the presence of colloidal  $^{68}\text{Ga}$ -species [24,25,27].

High-pressure liquid chromatography (HPLC) analysis was performed using an Agilent 1200 series HPLC (Wilmington, USA) instrument with a diode array UV detector. This system is coupled to a Gina Star Raytest (Strubenhardt, Germany) radio-detector. A reverse-phase X-Bridge C18 HPLC column (Waters, Milford, USA) with a 3.5  $\mu\text{m}$  particle size, 3.0mm x 100 mm was used for the radioanalysis in this investigation. The mobile phase consisted of solvent A (0.1% trifluoroacetic acid (TFA) in water and solvent B (0.1% TFA in acetonitrile). The system was operated at a linear A-B gradient with solvent B going from 5 - 95% over 20 minutes with a flow rate of 1 mL/min.

#### 4.2.5. Log P Octanol/Phosphate Buffered Assay

The method published by Jain and co-workers was used [28]. Briefly, 100  $\mu\text{l}$  ( $\pm$  100 MBq) of the labelled [ $^{68}\text{Ga}$ ]Ga-DOA-KP10 was dispersed in a 1 ml phosphate buffered saline (PBS) and octanol mixture (0.9:1). The samples were vortexed (1 min) and then centrifuged (5 min, 6000 rpm). A sample (200  $\mu\text{l}$ ) from each phase was taken and the activity measured in the Hidex AMG automated gamma counter (Turku, Finland). The partition coefficient (log P) was expressed as the logarithm of the ratio of counts from n-octanol fraction vs. that of the aqueous fraction [28,29].

#### 4.2.6. Ex Vivo Stability

The red blood cell (RBC) binding assay was performed by the method described by Shi and co-workers (2020). In brief, radiolabeled [ $^{68}\text{Ga}$ ]Ga-DOA-KP10 (740 kBq in 10  $\mu\text{l}$ ) was mixed with 100  $\mu\text{l}$

of human blood drawn up in the presence of heparin. The mixture was incubated in a shaking incubator at 37°C. Samples (200 µl each) were collected at two timepoints, 10 and 30 minutes. Plasma and blood cells were separated by centrifugation (2000 rpm, 5 minutes). The plasma was removed, and the blood cells were washed twice with 500 µl of normal saline (0.9% NaCl) which was then added to the plasma fraction. The amount (%) of labelled compound that was bound to the RBC was determined by the ratio of distribution between the plasma and blood cell fraction [29].

Stability studies were performed in triplicate using [<sup>68</sup>Ga]Ga-DOTA-KP10 spiked human serum, plasma or whole blood (samples were removed at 0, 60 minutes and 120 minutes with incubation at 37 °C). The [<sup>68</sup>Ga]Ga-DOTA-KP10 had a radiochemical purity of at least 95% purity (determined by HPLC analysis). The samples taken (200 µl) at the selected time points were treated with ice-cold acetonitrile (500 µl) and thereafter filtered with a 0.22 µm filter to remove all residual proteins in the extract. This sample was then analyzed by the HPLC method as described under Section 2.2.4. In vitro stability study data from [<sup>68</sup>Ga]Ga-DOTA-KP10 was deemed as translatable for [<sup>177</sup>Lu]Lu-DOTA-KP10 also since preliminary investigations demonstrated the same phenomena is present for both.

The protein binding assay was done as described by Mdlophane et al., (2020) [25]. In brief, [<sup>68</sup>Ga]Ga-DOTA-KP10 was incubated for 0, 30 minutes and 60 minutes in serum at 37 °C. Proteins were precipitated in ice-cold acetonitrile (500 µl) and centrifuged (5000 rpm, 10 minutes). The supernatant was removed, and the protein pellet was washed with acetonitrile (250 µl). The washed protein pellets and supernatants were measured in an automated gamma-counter (Hidex, Finland).

The bench-top stability of [<sup>68</sup>Ga]Ga-DOTA-KP10 was performed by keeping the final formulated radiopharmaceutical (RCP > 95%) at room temperature (approximately 25 °C) for a period of up to 120 minutes. This final formulation was buffered to a pH of 7 with PBS. Samples were collected at 30, 60 and 120 minutes. ITLC and HPLC analyses were performed as described earlier. For the formulated [<sup>177</sup>Lu]Lu-DOTA-KP10 (RCP > 95%), the bench-top stability analysis was performed at 24 hours.

#### 4.2.7. In Vivo Evaluation

All procedures followed during the animal studies adhered to institutional and South African national guidelines for the care and use of laboratory animals (SANS10386:2021). Ethical approval for the study was obtained from the Research Animal Ethics Committee of North-West University (NWU-00560-19-S5) and University of Pretoria (149/2019), South Africa. The animals were provided by the Department of Science and Technology/North-West University Preclinical Drug Development Platform (PCDDP) Vivarium. The study was conducted at the Preclinical Imaging Facility (PCIF) of the Nuclear Medicine Research Infrastructure (NuMeRI), South Africa. Five healthy Sprague-Dawley rats (male, 6-8 weeks, ± 200 grams) were enrolled into the study. All animals had ad libitum access to a conventional rodent diet and water. Animals were maintained on a 12-hour artificial day/night cycle and supplied with corn cob bedding and nesting material for cage enrichment. Environmental conditions were kept stable in individually ventilated cage system (Techniplast IVC, Milan, Italy). For imaging, rats were anaesthetized with an induction dose of 4 % of isoflurane in oxygen and maintained at 2% isoflurane in oxygen during the procedure. Image acquisition was done on a Mediso nanoPET/CT (Mediso, Hungary). The rats (n = 5) were administered intravenously with [<sup>68</sup>Ga]Ga-DOTA-KP10 (18,8 MBq ± 9.3 MBq) formulated in PBS to pH 7.0. The imaging protocol consisted of both a dynamic scan period (30-45 minutes) immediately following injection, as well as delayed image acquisition at 120-150 minutes post tracer injection. Dynamic images were regionally acquired: one bed position from the tip of the snout to below the diaphragm. Delayed whole body images were acquired over two bed positions. All list mode data acquired was corrected for scatter and randoms using Nucline™ software (version:2.01.020.0000; MEDISO, Hungary) using an iterative reconstruction algorithm with computed tomography (CT) attenuation correction maps. Hybrid images were viewed and analysed using InterviewFusion™ software (Mediso, Hungary). A qualitative visual analysis was done on all acquisitions, as well as delineation of volumes of interest (VOI) for all major internal structures to determine quantifiable biodistribution data.

#### 4.2.8. Ex-Vivo Biodistribution

A quantitative analysis of the radioactivity biodistribution and uptake in various organs of the rats was conducted. Following PET/CT imaging, the anesthetized animals were euthanized by

decapitation and blood was collected into pre-weighed BD SST vacutainer tubes (thermos Fisher Scientific, Johannesburg, South Africa). The blood samples were centrifuged (6000 rpm, 5 min) to separate the serum from blood cells. The blood and serum along with the other dissected tissues and organs (heart, liver, spleen, intestines, testes, stomach, lungs and brain) were weighed and the radioactivity measured in the automated gamma counter (Hidex AMG, Turku, Finland). The radioactivity per organ was expressed as the percentage injected dose per gram of the organ (% ID/g).

#### 4.2.9. Statistical Methods

All data analyses were performed with GraphPad Prism Software (Version 8.1 for Windows, GraphPad software, San Diego, California, USA). If not stated otherwise only data that has been executed at least in triplicate was considered relevant and was expressed as mean  $\pm$  standard error mean (SEM). A p-value of  $< 0.05$  was used to indicate statistical significance.

For the IP assay, the data was fitted using a non-linear regression to determine Emax and EC50. Data collected from the ex vivo biodistribution was evaluated using the Kruskal-Wallis, analysis. Chi-square that was less than the H-statistic was used to indicate significant differences between the concentrations within regions of interest. Organs were measured for activity and expressed as the percentage injected dose per gram of the organ (%ID/g). The Mann-Whitney u-test was performed by comparing the mean %ID/g of the respective organ of interest to the control groups organ mean % ID/g to determine whether the mean activity measurements were different. A multipoint regression model (exponential fit) was used to estimate blood-half life.

## 5. Conclusions

A KISS1R targeting construct (DOTA-KP-10) was designed, radiolabeled, and tested in healthy mice for further development as a new potential theranostic radiopharmaceutical. This ligand demonstrated the expected behavior for DOTA complexes during radiolabeling. DOTA-KP-10 was conjugated to DOTA via the NH<sub>2</sub> terminal and labelled with gallium-68 and lutetium-177. Gallium-68 and lutetium-177 were selected in view of their wide availability, as well as for their excellent properties as theranostic radionuclide pair. Importantly, the radiosynthesis steps utilized did not require labor intensive equipment such as a preparative HPLC purification.

Whilst showing excellent radioisotope complexation and peptide stability in aqueous solvents, the radiopharmaceutical demonstrated a degree of instability in vitro which may be subject to further improvements based on structure-activity relationship studies to decipher a balanced design for maintained receptor affinity paired with desired proteolytic resistance. The preliminary in vivo assays in healthy animals showed good blood clearance for the radiopharmaceutical within 45 minutes. The relatively rapid blood clearance is advantageous if this compound is to be applied to tumor imaging.

In view of both negative and positive putative roles of kisspeptin in various cancers the visualization of the KISS1R in oncology constitutes an interesting and multidimensional radiopharmaceutical across many tumor types.

**Supplementary Materials:** The following supporting information can be downloaded at: [www.mdpi.com/xxx/s1](http://www.mdpi.com/xxx/s1), Figure S1: title; Table S1: title; Video S1: title.

**Author Contributions:** Conceptualization, MS, JRZ, TE and RPM ; methodology, JK, MS, JRZ, TE, RPM; validation, CHSD and BMP; formal analysis, RR, CHSD and BMP; investigation, JK, RR, CHSD, BMP and TE; resources, JRZ, TE, RPM and MS; data curation, JK, RR, CHSD and BMP; writing—original draft preparation, JK, RR, and TE; writing—review and editing, MS, JRZ, TE, RPM; visualization, JK, CHSD and BMP; supervision, MS, JRZ, TE, and RPM; project administration, MS, JRZ, TE, and RPM. All authors have read and agreed to the published version of the manuscript.

**Funding:** This research received no external funding.

**Institutional Review Board Statement:** All procedures followed during the animal studies adhered to institutional and South African national guidelines for the care and use of laboratory animals (SANS10386:2021). Ethical approval for the study was obtained from the Research Animal Ethics Committee of North-West University (NWU-00560-19-S5) and University of Pretoria (149/2019), South Africa.

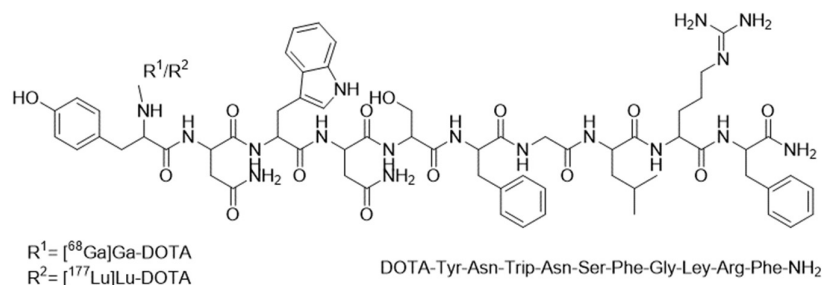
**Informed Consent Statement:** Not applicable.

**Data Availability Statement:** The data that support the findings of this study are available on request from the corresponding author Robert P. Millar.

**Acknowledgments:** The authors would like to thank Ms. Delene van Wyk and Ms. Cecile Swanepoel for technical assistance with image acquisition and processing, Ms. Jillene Visser and Dr. Nico Minaar for veterinary oversight and assistance. The authors further thank Ms. Palesa Koatale for her assistance and Dr. Zulfiyah Mohamend Moosa for scientific advice. Illustrations were created by Janke Kleynhans using licensed software (BioRender®, GraphPad Prism).

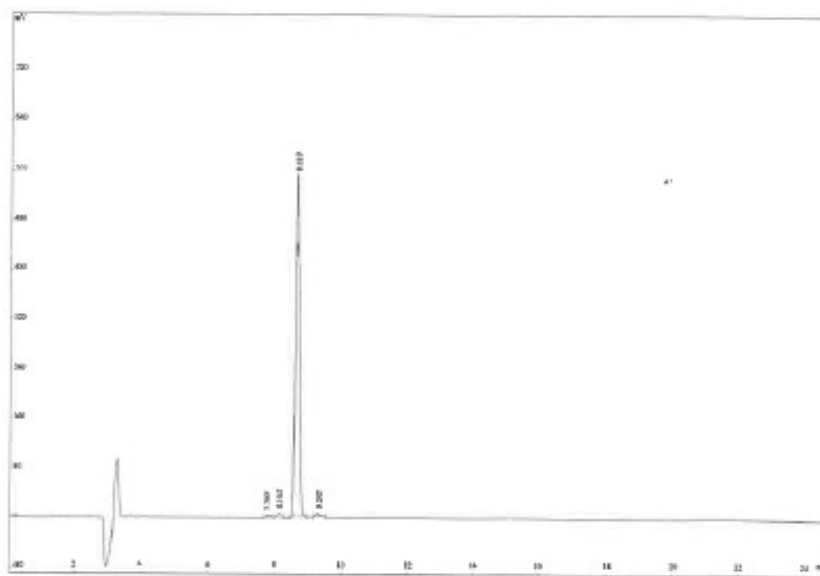
**Conflicts of Interest:** The authors declare no conflicts of interest.

#### Appendix A. Structure of DOTA-KP10



#### Appendix B. HPLC Dat of Raw Material DOTA-KP10

Column, 4.6 x 250 mm, Kromasil 100-5-C18. Solvent A 0.1% TFA in 100% Acetonitrile, Solvent B, 0.1% TFA in 100% Water. Flow rate 1.0 ml/min. Wavelength 220 nm, Volume 5 µl. 0.01 min A 29%, B 71%; 25 min A 54%, B 46%, 25.1 min A 100%, B 0%, 30 min STOP.

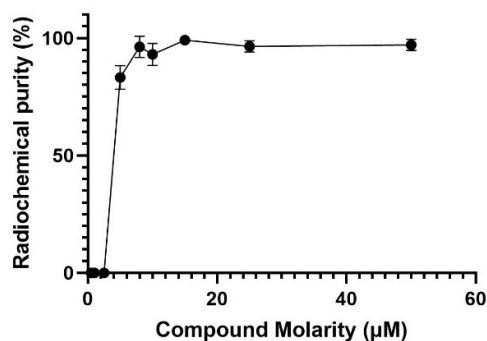


Rank	Time	Conc.	Area	Height
1	7.760	1.011	46202	4540
2	8.104	1.158	52919	6979
3	8.619	96.47	4407608	568551
4	9.245	1.362	62235	6857

## Appendix C

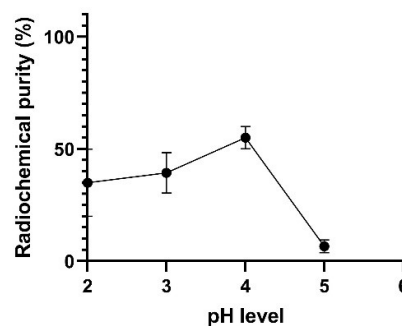
The optimization of  $^{68}\text{Ga}$ -labelling of DOTA-KP10 was performed with different compound molarities ranging from 2.5  $\mu\text{M}$  to 25  $\mu\text{M}$  and the results are provided in Figure 3A.  $^{68}\text{Ga}$ -radiolabelling became more quantitative at 7.5  $\mu\text{M}$  (N=3) with robust labelling results obtained using 10  $\mu\text{M}$  of DOTA-KP10 for the radiosynthesis. The pH range investigated was from 2.0 to 5.0 with labelling being considered optimal at a pH of 4.0 (Figure 3B). Colloidal gallium-68, as well as free gallium-68, was present at pH 3 and lower and other colloidal species become problematic at pH 5. Incubation times were evaluated from start of synthesis up to 20 minutes at various temperatures (room temperature, 60  $^{\circ}\text{C}$  and 95 $^{\circ}\text{C}$ ) (Figure 3C). Quantitative labelling was achieved at 95  $^{\circ}\text{C}$  after 10 minutes of incubation time. For labelling of DOTA-KP10 with lutetium-177, only the compound molarity was investigated (Figure 3D).

3A: Effect of compound molarity on gallium-68 labelling



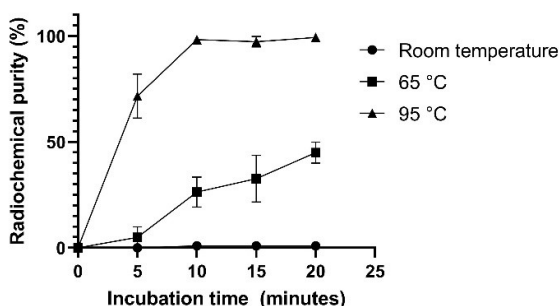
(a)

3B: Effect of pH on gallium-68 labelling



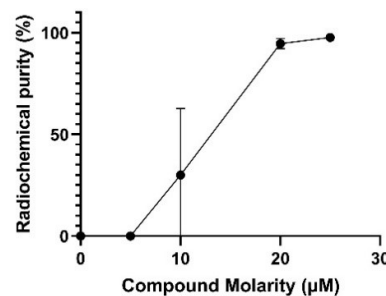
(b)

3C: Effect of incubation time and temperature on gallium-68 labelling



(c)

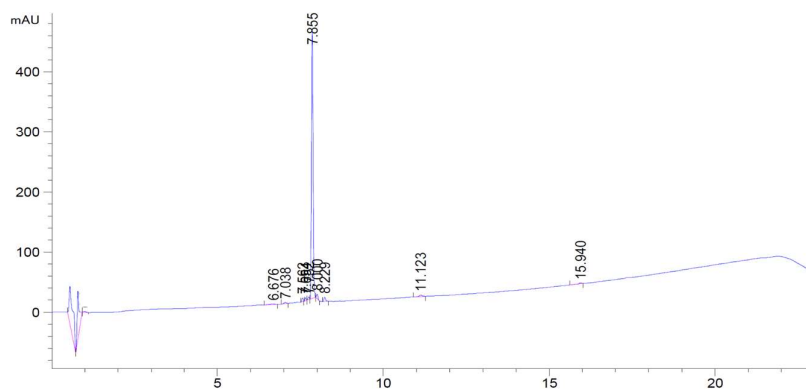
3D: Effect of compound molarity on lutetium-177 labelling



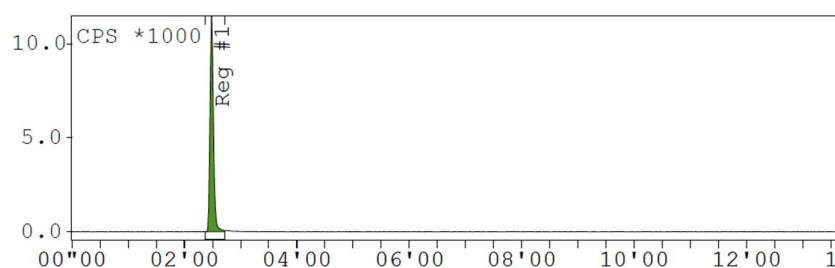
(d)

**Figure 3.** The effects of various parameters on the radiolabelling efficiency of gallium-68 and compound molarity of lutetium-177 with DOTA-KP10. A) The effect of compound molarity B) the effect of pH on  $^{68}\text{Ga}$ -complexation, C) The effects of temperature and incubation time on  $^{68}\text{Ga}$ -product yield and D) the effect of compound molarity on  $^{177}\text{Lu}$ -labelling.

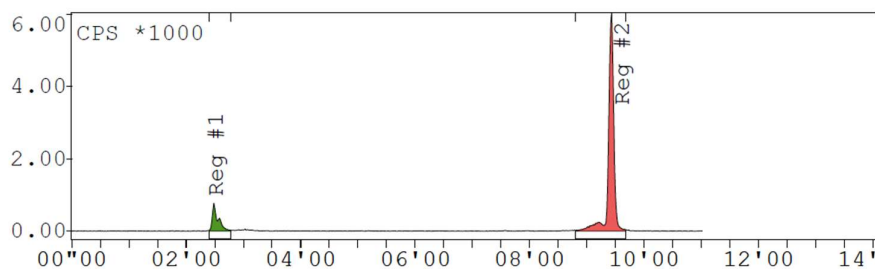
## Appendix D. Chromatogram Examples



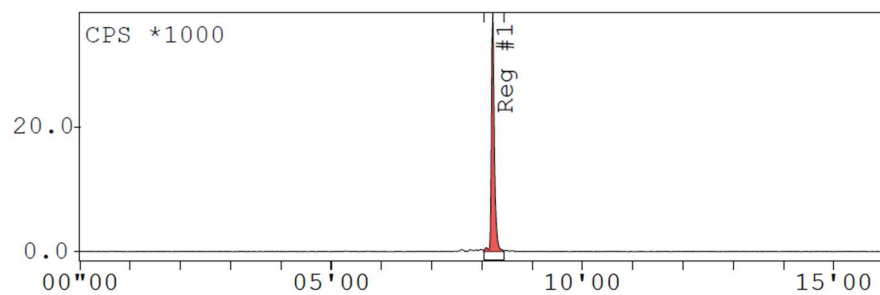
UV determination of retention time of unlabelled DOTA-KP-10 with the signal positioned at 7.8 minutes and the method run for 20 minutes. This was performed with unlabelled DOTA-KP10



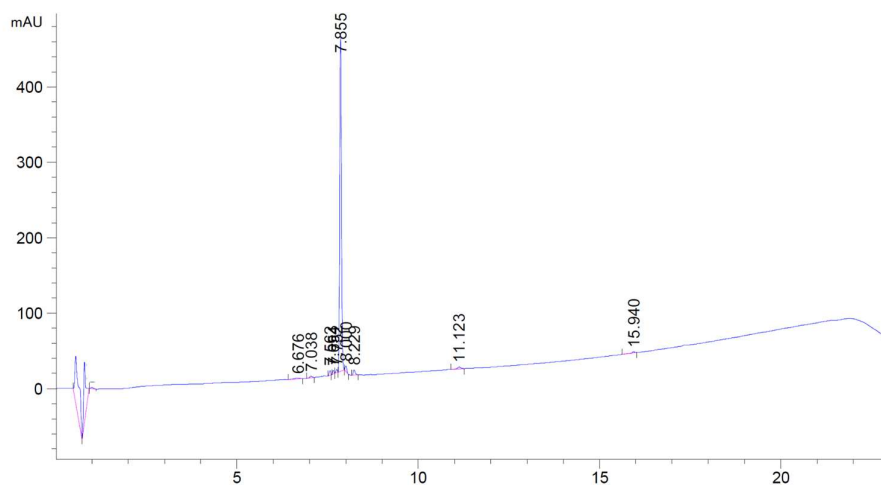
Radiochemical purity of 0% with only free gallium-68 present in the sample.



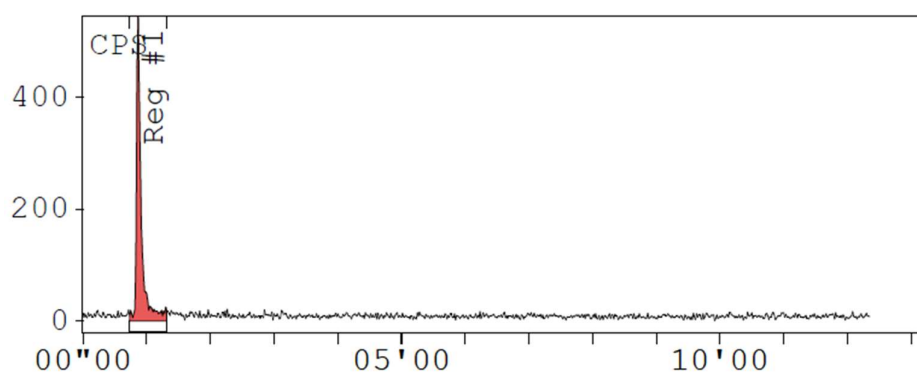
Radiochromatogram of radiolabelling in suboptimal reaction conditions resulting in a radiochemical purity of less than 95%.



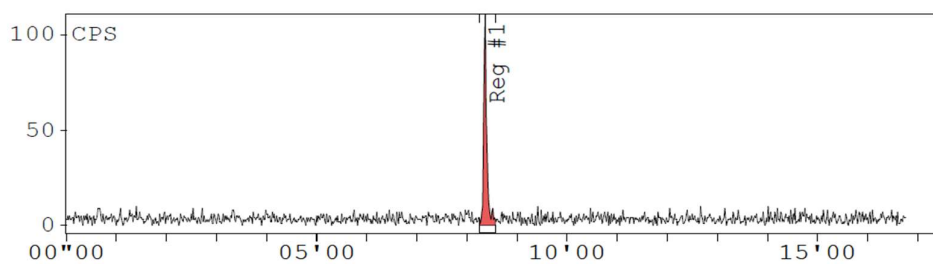
Radiochromatogram of a radiolabelling performed in optimal reaction conditions resulting in a radiochemical purity of more than 95%. Note the retention time of [<sup>68</sup>Ga]Ga-DOTA-KP10 at 8.2 minutes.



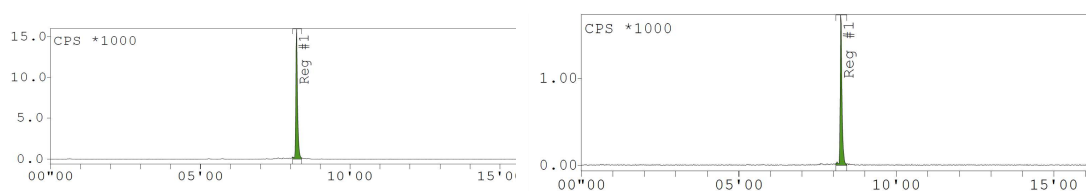
UV determination of retention time of unlabelled DOTA-KP-10 with the signal positioned at 7.8 minutes and the method run for 20 minutes. This was performed with unlabelled DOTA-KP10

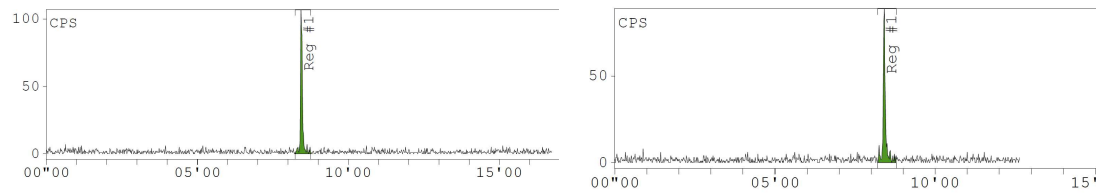
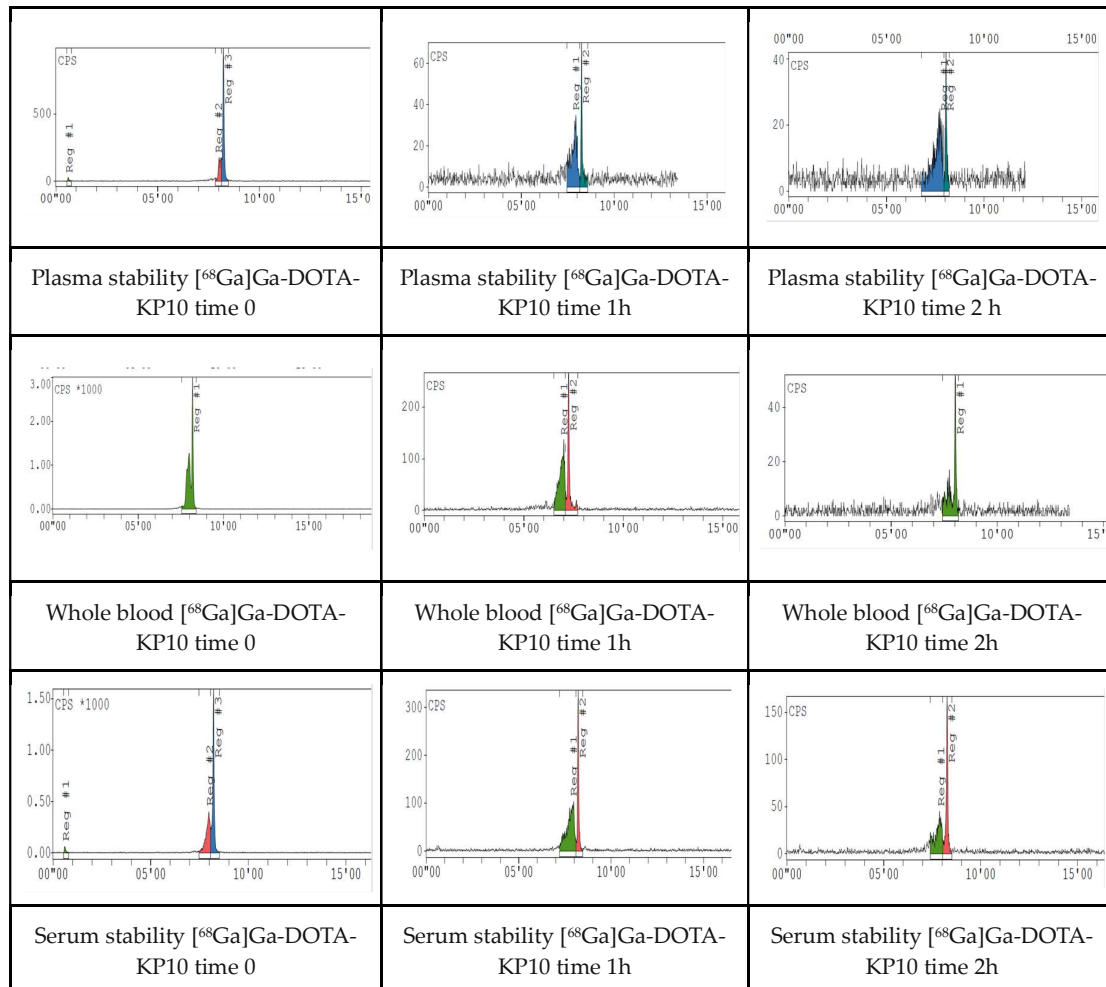


Radiochemical purity of 0% with only free lutetium-177 present in the sample.



Radiochromatogram of a radiolabelling performed in optimal reaction conditions resulting in a radiochemical purity of more than 95%. Note the retention time of [ $^{177}\text{Lu}$ ]Lu-DOTA-KP10 at 8.2 minutes.



[<sup>68</sup>Ga]Ga-DOTA-KP-10 Time 0 and time 3 hours bench -top Stability[<sup>177</sup>Lu]Lu-DOTA-KP-10 Time 0 and Time 24 hours bench-top stability

## References

1. Ciaramalla, V., Della Corte, C.M., Ciardiello, F., Morgillo, F. Kisspeptin and Cancer: Molecular interaction, biological functions, and future perspectives. *Front Endocrinol* **2018**, *9*, 115. DOI: DOI:10.3389/fendo.2018.00115.
2. Guzman, S., Brackstone, M., Radovick, S., Badwah, A.V., Bhattacharya, M.M. KISS1/KISS1R in cancer: friend or foe? *Front Endocrinol* **2018**, *9*, 437. DOI: 10.3389/fendo.2018.00437.
3. Blake, A., Dragan, M., Tirona, R.G., Hardy, D.B., Brakstone, M., Truck, A.B., Badwah, A.V., Bhattacharya, M.G. G protein-coupled KISS1 Receptor is overexpressed in triple negative breast cancer and promotes drug resistance. *Sci Rep* **2017**, *7*, 46525. DOI: 10.1038/srep46525.
4. Frantagelo, F., Carroerop, M.V., Motti, M.L. Controversial role of kisspeptins/KISS-1R signalling system in tumour development. *Front Endocrinol* **2018**, *9*, 192. DOI: 10.3389/fendo.2018.0192.

5. Dragan, M., Nguyen, M.U., Guzman, S., Goertzen, B., Brackstone, M. G-protein coupled kisspeptin receptor induces metabolic reprogramming and tumorigenesis in oestrogen receptor-negative breast cancer. *Cell Death Dis* **2020**, *11*, 206. DOI: 10.1038/s47419-020-2305-7.
6. Stathaki, M., Stamatou, M.E., Magioris, G., Simantaris, S., Syroigos, N. et al. The role of kisspeptin system in cancer biology. *Crit Rev Oncol Hematol* **2019**, *142*, 130-140. DOI: 10.1016/j.cretrevonc.2019.07.015.
7. Loosen, S.V., Luedde, M., Lurie, G., Spehlmann, M., Paffenholz, P., Ulmer T.F. et al. Serum levels of kisspeptin are elevated in patients with pancreatic cancer. *Disease Markers* **2019**, 5603474. DOI: 10.1155/2019/5603474.
8. Xoxakos, I., Petraki, C., Msaouel, P., Armakolas, A., Grigorakis, A., Stefanakis, S., Koutsilieris, M. Expression of Kisspeptin (KISS1) and its receptor GPR54 (KISS1R) in prostate cancer. *Anticancer Res* **2020**, *40*(2), 709-718. DOI: 10.21876/anticancer.14001.
9. Banerjee Sr, Pamper, M.G. Clinical applications of gallium-68. *Appl Radiat Isotopes*, **2013**, *76*, 2-13. DOI: 10.1016/j.apradiso.2013.01.039.
10. Spang, P., Herrmann, C., Roesch, F. Bifunctional gallium-68: past, present and future. *Semin Nucl Med* **2016**, *46*, 373-394. DOI: 10.1543/j.semnuclmed.2016.04.003.
11. Baranvai, Z., Tircso, G., Roesch, F. The use of the macrocyclic chelator DOTA in radiochemical preparations. *Eur J Inorg Chem* **2020**, *1*, 36-56. DOI: 10.1002/ejic.201900706.
12. Rather, M.A., Basha, S.H., Bhat, I.A., Sharma, N., Nandanpawar, P. Characterization, molecular docking, dynamics simulation and metadynamics of kisspeptin receptor with kisspeptin. In *J Biol Macromol* **2017**, *101*, 241-253. DOI: 10.1016/j.ijbiomac.2017.03.102.
13. Roseweir, A.K., Millar, R.P. Kisspeptin antagonists. *Adv Exp Med Biol* **2013**, *784*, 159-186. DOI: 10.1007/978-1-4614-6199-9\_8.
14. Paquier, J., Kamech, et al. Molecular evolution of GPCRS: kisspeptin/kisspeptin receptors. *J Mol Endocrinol* **2014**, *52*, 3. DOI: 10.1530/JME-13-0224.
15. Jain, A., Chakraborty, S., Sharma, H.D., Dash, A. A systematic comparative evaluation of [<sup>68</sup>Ga]Ga-labelled RGD peptides conjugated with different chelators. *Nucl Med Mol Imaging* **2018**, *52*, 152-134. DOI: 10.1007/s13139-017-0499-0.
16. EDQM. European pharmacopoeia 8.0. Radiopharmaceutical preparation; gallium octreotide. European directorate for the quality Medicines, Strasbourg pp 1061-1064.
17. Asami, T., Nishizawa, N., Ishibashi, Y., Nishibori, K., Nakayama, M. et al. Serum stability of selected decapeptide agonists of KISS1R using pseudopeptides. *Bioorganic Med Chem Lett* **2012**, *22*, 6391-6396. DOI: 10.1016/j.bmcl.2012.08.069.
18. Robinson, A.B., Mckerrow, J.H., Cary, P. Controlled deamidation of peptides and proteins: an experimental hazard and a possible biological timer. *PNAS* **1970**, *66*, 753-757. DOI: 10.1073/pnas.66.3.753.
19. Robinson, N.E., Robinson, Z.W., Robinson, B.R., Robinson, A.L., Robinson, J.A., Robinson, M.L., Robinson, A.B. Structure-dependant nonenzymatic deamidation of glutaminyl and asparaginyl pentapeptides. *J Pept Res* **2004**, *63*, 426-436. DOI: 10.1111/j.1399-3011.2004.00151.x.
20. Asami, T., Nischizawa, N., Matsui, H., Nishibori, K., Ishibashi, Y., Horikoshi, Y., Nakayama, M., Mastumoto H et al. Design, synthesis and biological evaluation of novel investigational nonpeptide KISS1R agonists with testosterone-suppressive activity. *J Med Chem* **2013**, *56*, 8298-8307. DOI: 10.1021/jm401056w.
21. Asami, T., Nischizawa, N., Ishibashi, Y., Nishibori, K., Nakayama, M., Horikoshi, Y., Matsumoto, S.I., Yamaguchi, M et al. Serum stability of selected decapeptide agonists of KISS1R using pseudopeptides. *Bioorg Med Chem Lett* **2012**, *22*, 6391-6396. DOI: 10.1016/j.bmcl.2012.08.069.
22. Newton, C.L., Anderson, R.C., Katz, A.A., Millar, R.P. Loss of function mutations in the human luteinizing hormone receptor predominantly cause intracellular retention. *Endocrinol* **2016**, *157*, 4364-4377. DOI: 10.1210/en.2016-1104.
23. Hanyroup, S., Anderson, R.C., Nataraja, S. Yu, H.N., Millar, R.P., Newton, C.L. Rescue of cell surface expression and signalling of mutant follicle-stimulating hormone receptors. *Endocrinol* **2021**, *162*,12. DOI: 10.1210/endo/bqab134.
24. Ebenhan, T., Chadwick, N., Sathekge, M.M., Govender, P., Kruger, T., Marjanovic-Painter, B., Zeevaart, J.R., Peptide synthesis, characterization and <sup>68</sup>Ga-radiolabelling of NOTA-conjugated ubiquicidin fragments for prospective infection imaging with PET/CT. *Nucl Med Biol* **2014**, *41*, 390-400. DOI: 10.1016/j.nucmedbio.2014.02.001.
25. Mdlophane, A.H., Ebenhan, T., Marjanovic-Painter B, Govender, T., Sathekge, M.M., Zeevaart, J.R. Comparison of DOTA and NODAGA as chelates for <sup>68</sup>Ga-labelled CDP1 as novel infection PET imaging agents. *J Radioanal and Nucl Chem* **2019**, *322*, 629-638. DOI: 10.1007/s10967-019-06639-5.
26. Sinnes, J., Nagel, J., Roesch, F. AAZTA5/AAZTA5-TOC: synthesis and radiochemical evaluation with <sup>68</sup>Ga, <sup>44</sup>Sc and <sup>177</sup>Lu. *EJNMMI Radiopharm & Radiochem* **2019**, *4*, 18. DOI: 10.1186/s41181-019-0068-1.
27. De Blois, E., Sze, C.E., Naidoo, C., Prince, D., Krennig, E.P., Breeman, W.A.P. Characteristics of SnO<sub>3</sub> based <sup>68</sup>Ge/<sup>68</sup>Ga generator and aspects of radiolabeling DOTA-peptides. *Appl Radiat Isot* **2011**, *69*, 308-315. DOI: 10.1016/j.apradiso.2010.11.015.

28. Jain, A., Kameswaran, M., Pandey, U., Sarma, H.D., Dash, A. 68Ga-labelled erlotinib: a novel PET probe for imaging EGRF over-expressing tumours. *Bioorgan Med Chem Lett* **2017**, *27*, 4552-4557. DOI: 10.1016/j.bmcl.2017.08.065.
29. Shi, S., Zhang, L., Wu, Z., Zhang, A., Hong, H., Choi, S.R., Zhu, L., Kung, H.F. [68Ga]Ga-HBED-CC-DiAsp: a new renal function imaging agent. *Nucl Med Biol* **2020**, *82-83*, 17-24. DOI: 10.1016/j.nucmedbio.2019.12.005.

**Disclaimer/Publisher's Note:** The statements, opinions and data contained in all publications are solely those of the individual author(s) and contributor(s) and not of MDPI and/or the editor(s). MDPI and/or the editor(s) disclaim responsibility for any injury to people or property resulting from any ideas, methods, instructions or products referred to in the content.